Supplementary Material for:

Thermal conductivity of $(Ge_2Sb_2Te_5)_{1-x}C_x$ phase change films

Ethan A. Scott,[1,2] Elbara Ziade,[1] Christopher B. Saltonstall,[1] Anthony E. McDonald,[1] Mark A. Rodriguez,[1] Patrick E. Hopkins,[2,3,4] Thomas E. Beechem,[1,5] and David P. Adams[1]

[1)]*Sandia National Laboratories, Albuquerque, NM 87185, USA*

[2)]*Department of Mechanical and Aerospace Engineering, University of Virginia, Charlottesville, VA 22904, USA*

[3)]*Department of Materials Science and Engineering, University of Virginia, Charlottesville, VA 22904, USA*

[4)]*Department of Physics, University of Virginia, Charlottesville, VA 22904, USA*

[5)]*Center for Integrated Nanotechnologies, Albuquerque, NM 87185, USA*

CONTENTS

S1. WHITE LIGHT INTERFEROMETRY

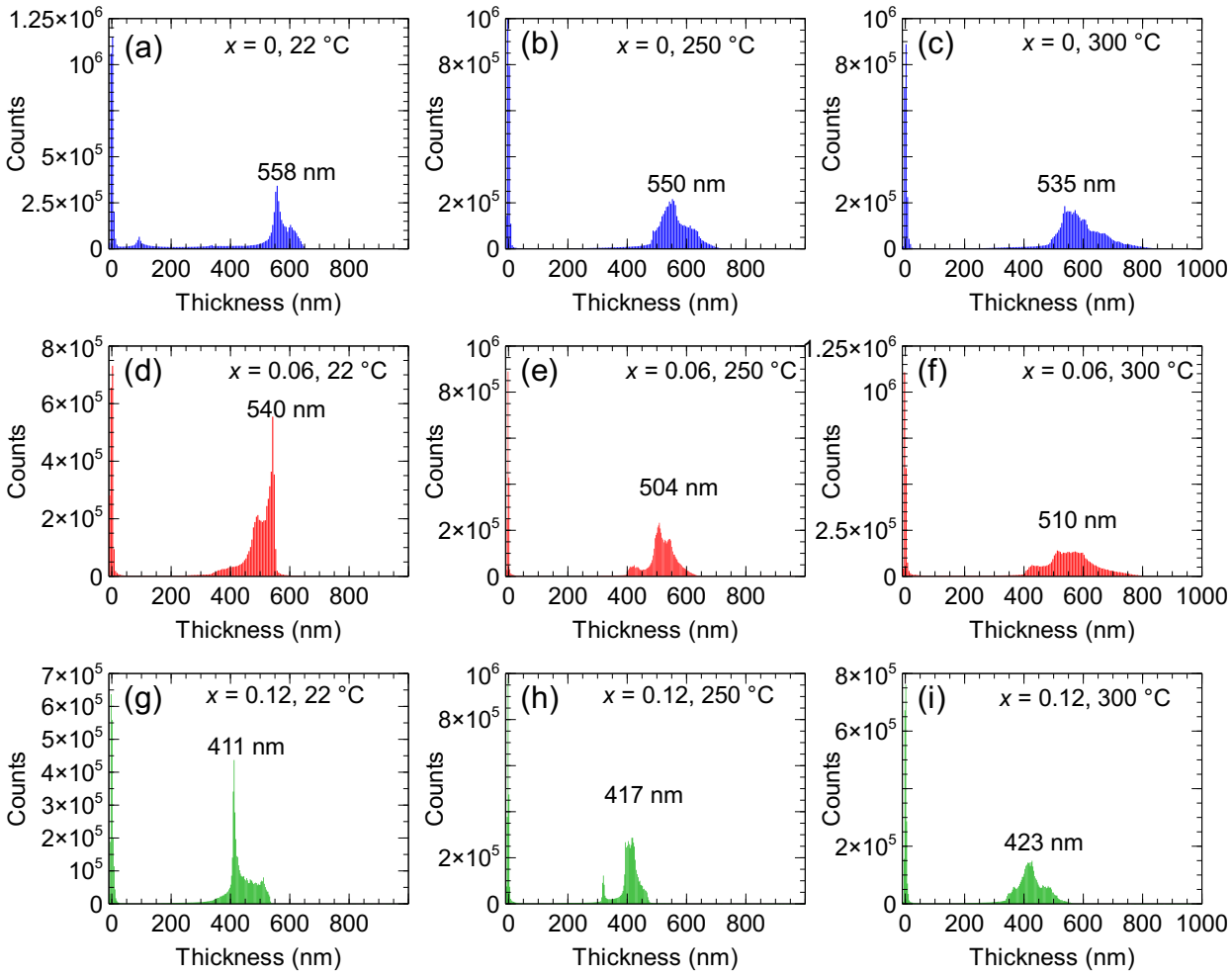

FIG. S1. Histograms produced from thickness contours measured with white light interferometry.

For thermal analysis, white light interferometry was employed to determine the thickness distribution for select films for x = 0, 0.06, and 0.12. Prior to $(Ge_2Sb_2Te_5)_{1-x}C_x$ film deposition, one quadrant of the sample was masked to provide an area distinguishable from the coated film. Thickness contours from the white light interferometry measurements were subsequently binned into histograms, from which the average peak position was taken as the average film thickness. For each composition, the average film thickness (among films annealed at different temperatures) was taken as the thickness for subsequent thermal analysis.

S2. SENSITIVITY ANALYSIS

In consideration of the thermal model and parameter sensitivity, we provide example model fits in Figures S2(a,b) and S3(a,b) and sensitivity calculations in S2(c,d) and S3(c,d). In this example, the data shown is from a sample of $(Ge_2Sb_2Te_5)_{0.94}C_{0.06}$ annealed at 50 °C. Figure S2 illustrates the sensitivity to the Au/Ti and $(Ge_2Sb_2Te_5)_{1-x}C_x$ interface by considering two extreme values in thermal boundary conductance, 10 and 1000 MW m^{-2} K^{-1}. In either case, there is limited effect on the fitted values for the volumetric heat capacity and thermal conductivity of the film, with the nominal fitted values being within uncertainty of each other. This is illustrated by the lack of sensitivity to the value of the interface, as seen in Figures S2(a,b). The same apporach is used for insight into the sensitivity of the $(Ge_2Sb_2Te_5)_{1-x}C_x/SiO_2$ interface in which a similar result is found, in that there is little sensitivity to the back side conductance. The material parameters used to create the sensitivity plots are tabulated in Tables S1 and S2.

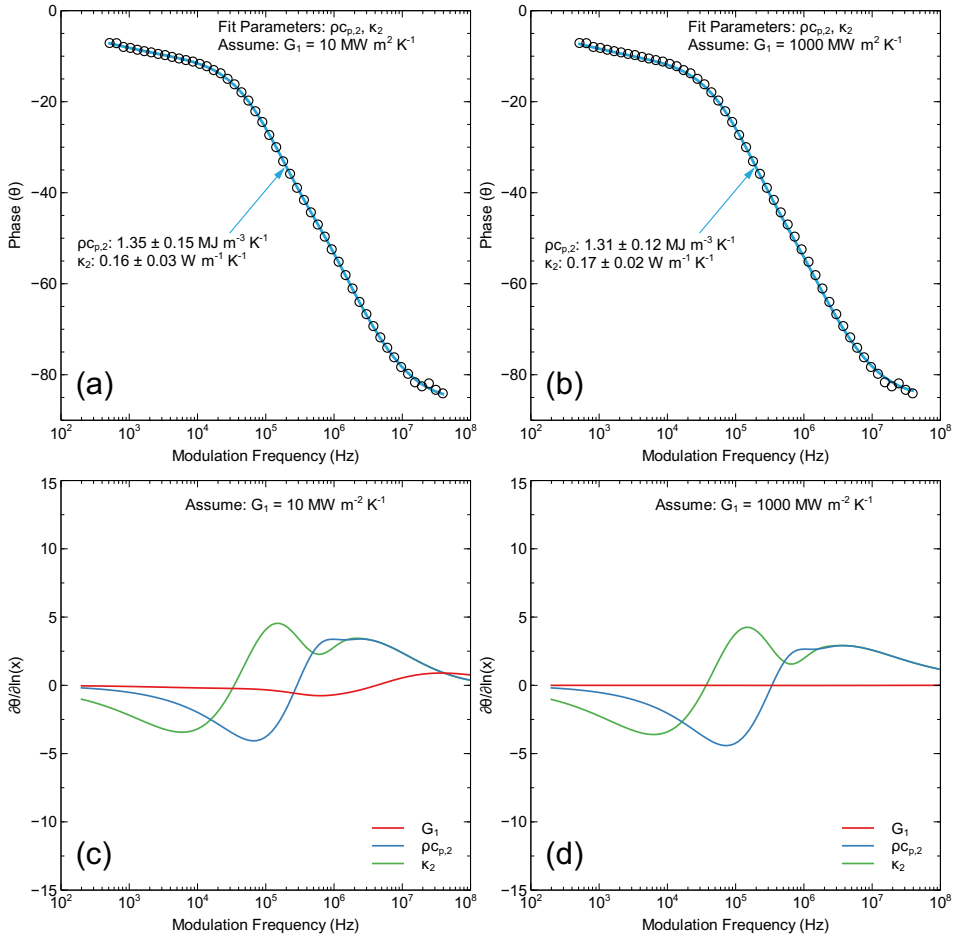

FIG. S2. Example model fits (a,b) and corresponding fitted parameter sensitivity (c,d) assuming different values for the Au/Ti and $(Ge_2Sb_2Te_5)_{1-x}C_x$ interface. In this case, the example fit is of $(Ge_2Sb_2Te_5)_{0.94}C_{0.06}$ annealed at 50 °C.

Layer	ρc_p (MJ m^{-3} K^{-1})	κ (W m^{-1} K^{-1})	d (nm)	G (MW m^{-2} K^{-1})
Au/Ti	2.48	147	128	10-1000
$(Ge_2Sb_2Te_5)_{1-x}C_x$	fit	fit	510	1000
SiO_2	1.65	1.3	semi-inf.	N/A

TABLE S1. Values used to for the sensitivity calculation in Figure S2.

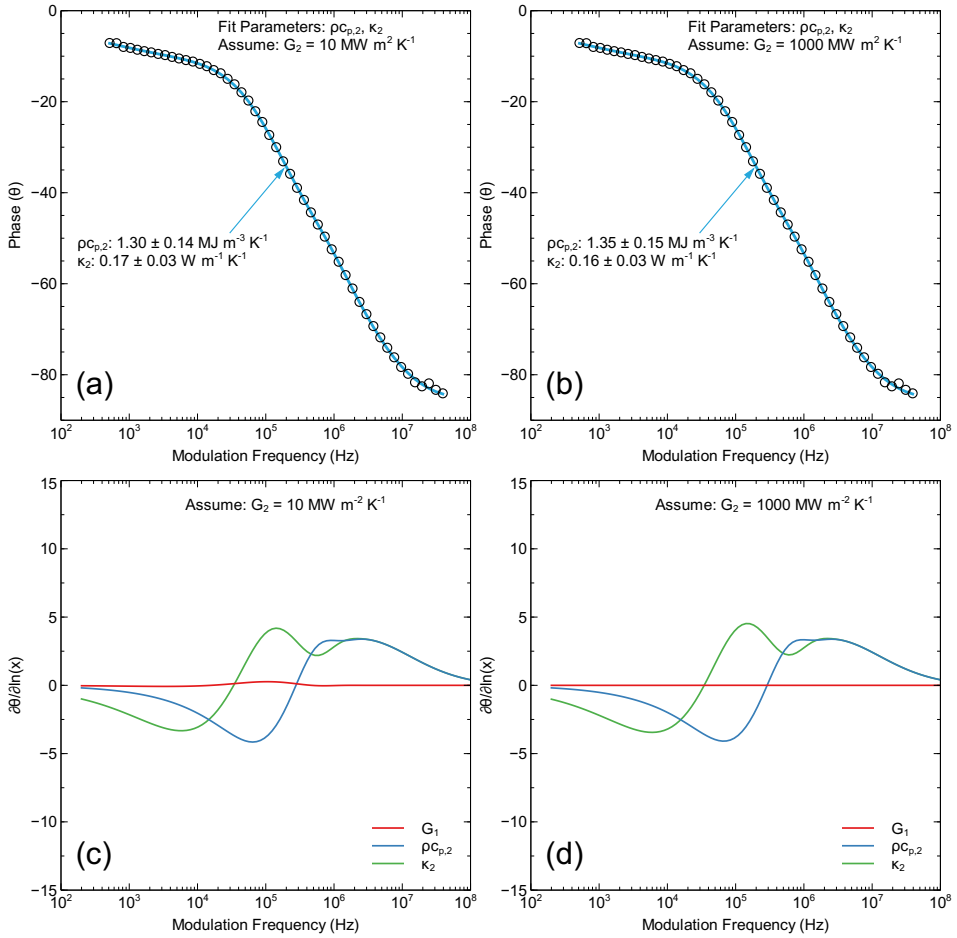

FIG. S3. Example model fits (a,b) and corresponding fitted parameter sensitivity (c,d) assuming different values for the $(Ge_2Sb_2Te_5)_{1-x}C_x$ and SiO_2 interface. In this case, the example fit is of $(Ge_2Sb_2Te_5)_{0.94}C_{0.06}$ annealed at 50 °C.

Layer	ρc_p (MJ m^{-3} K^{-1})	κ_{perp} (W m^{-1} K^{-1})	d (nm)	G (MW m^{-2} K^{-1})
Au/Ti	2.48	147	128	10
$(Ge_2Sb_2Te_5)_{1-x}C_x$	fit	fit	510	10-1000
SiO_2	1.65	1.3	semi-inf.	N/A

TABLE S2. Values used to for the sensitivity calculation in Figure S3.

S3. THERMAL CONDUCTIVITY CALCULATIONS

As both the structural and electronic properties are subject to changes in carbon concentration, we consider the comprehensive effects in a similar manner as prior reports[1,2], in that the measured thermal conductivity can be considered as an aggregate of the electron and phonon contributions to the total thermal conductivity:

$$\kappa_{measured} = \kappa_e + \kappa_{ph}, \tag{S1}$$

where κ_e and κ_{ph} are the electron and phonon contributions to the total measured thermal conductivity, $\kappa_{measured}$, as determined by FDTR. The electronic contribution to thermal conductivity can be calculated from the resistivity measurements through the Wiedemann-Fraz Law, in that

$$\kappa_e = LT\rho^{-1}, \tag{S2}$$

where L is the Lorenz number, T is the temperature of the material, and ρ is the resistivity of the film. We note that for these calculations, a slightly different value for ρ is utilized compared to that displayed in Fig. 1(c) of the main manuscript; this is because films used for resistivity measurements had a slightly different thickness than those prepared for thermal measurement. Therefore, we assume the same sheet resistance measured from four-point probe measurement, but use the thickness of the films used for thermal measurement, determined through white light interferometry. To account for potential variation in the Lorenz number, we bound our calculations by considering Lorenz numbers spanning from 1.5 - 2.44$\times 10^{-8}$ W Ω K^{-2}, which provides a range representative of semiconductor materials[3]. The Sommerfeld value of the Lorenz number serves as an upper bound, and is routinely applied for $Ge_2Sb_2Te_5$[4–7], including films in the amorphous phase[1,8], as well as for compositions of $Ge_2Sb_2Te_5$ with a quaternary addition[8]. A lower bound of 1.5$\times 10^{-8}$ W Ω K^{-2} is considered as a converged limit for non-degenerate semiconductors[9], and has also been applied in several prior papers considering the electronic contribution to thermal conductivity in $Ge_2Sb_2Te_5$[3,10].

The phonon contribution to the thermal conductivity can therefore be determined by subtracting the electrical component from $\kappa_{measured}$. In the main manuscript, we contrast the values determined from experimental data with theoretical values as calculated from the lower limit to thermal conductivity as detailed by Cahill, Watson, and Pohl[11]. This model considers phonon transport within amorphous materials and disordered crystals as a random walk of energy between harmonic oscillators which encounter scattering events separated by distances equal to one half the

period of vibration. For temperatures greater than the Debye temperature (which is approximately 100 K for $Ge_2Sb_2Te_5$[12]), the limit can be simplified as

$$\kappa_{ph,min} = \frac{1}{2}\left(\frac{\pi}{6}\right)^{\frac{1}{3}} k_B n_a^{\frac{2}{3}} (v_l + 2v_t), \tag{S3}$$

where k_B is the Boltzmann constant, n_a is the atomic density, and v_l and v_t are the longitudinal and transverse sound speeds within the film[1,2]. Due to close similarity in measured thermal conductivity of the non-carbon $Ge_2Sb_2Te_5$ measured in this work and that of Lyeo *et al.*[2], we apply those values for atomic density and sound speed, and assume similar values for the films with added carbon (n_a = 3.09×10^{22} cm^{-3}, $v_t = 2250, 3190, 3300$ m/s for the amorphous, fcc, and trigonal phases, respectively, and $v_l = 0.6v_t$). A weighted mean is then used to sum the calculated phonon contributions to thermal conductivity for each phase according to the corresponding fractional phase composition, which is determined from PCA analysis. For reference, the values used in the thermal calculations are tabulated in Table S3.

x	Anneal Temperature (°C)	ρ (Ω m)	$\kappa_{measured}$
0	22	1.23E+01	0.18
	50	6.82E+00	0.18
	100	9.02E+00	0.18
	150	1.33E-03	0.47
	200	1.09E-04	0.67
	250	4.22E-05	0.74
	300	1.50E-05	1.20
0.06	22	2.02E+01	0.17
	50	2.05E+01	0.16
	100	1.55E+01	0.17
	150	5.24E-03	0.35
	200	1.41E-03	0.39
	250	2.01E-04	0.39
	300	1.41E-05	0.95
	350	1.07E-05	1.09
0.12	22	3.70E+01	0.16
	50	6.74E+01	0.17
	100	9.70E+01	0.16
	150	1.29E+02	0.15
	200	2.61E+01	0.14
	250	1.75E-01	0.15
	300	1.02E-03	0.25
	350	6.62E-05	0.43

TABLE S3. Tabulated data for the nominal values used for calculations of the phonon and electronic components of thermal conductivity as well as the results of the minimum limit calculation from Equation S3.

REFERENCES

[1]J. Lee, E. Bozorg-Grayeli, S. Kim, M. Asheghi, H.-S. Philip Wong, and K. E. Goodson, Appl. Phys. Lett. **102**, 191911 (2013).

[2]H.-K. Lyeo, D. G. Cahill, B.-S. Lee, J. R. Abelson, M.-H. Kwon, K.-B. Kim, S. G. Bishop, and B.-k. Cheong, Appl. Phys. Lett. **89**, 151904 (2006).

[3]W.-X. Song, Y. Cheng, D. Cai, Q. Tang, Z. Song, L. Wang, J. Zhao, T. Xin, and Z.-P. Liu, J. Appl. Phys. **128**, 075101 (2020).

[4]D. Campi, E. Baldi, G. Graceffa, G. C. Sosso, and M. Bernasconi, J. Phys.: Condens. Matter **27**, 175009 (2015).

[5]X. Cai and J. Wei, in *2012 International Workshop on Information Storage and Ninth International Symposium on Optical Storage*, Vol. 8782, edited by F. Gan and Z. Song, International Society for Optics and Photonics (SPIE, 2013) pp. 142 – 147.

[6]A. Faraclas, G. Bakan, L. Adnane, F. Dirisaglik, N. E. Williams, A. Gokirmak, and H. Silva, IEEE Trans. Electron Devices **61**, 372 (2014).

[7]A. Vora-ud, M. Rittiruam, M. Kumar, J. G. Han, and T. Seetawan, Mater. Des. **89**, 957 (2016).

[8]W. P. Risk, C. T. Rettner, and S. Raoux, Appl. Phys. Lett. **94**, 101906 (2009).

[9]H.-S. Kim, Z. M. Gibbs, Y. Tang, H. Wang, and G. J. Snyder, APL Mater. **3**, 041506 (2015).

[10]R. Lan, R. Endo, M. Kuwahara, Y. Kobayashi, and M. Susa, J. Electron. Mater. **47**, 3184 (2018).

[11]D. G. Cahill, S. K. Watson, and R. O. Pohl, Phys. Rev. B **46**, 6131 (1992).

[12]J. Lee, Z. Li, J. P. Reifenberg, S. Lee, R. Sinclair, M. Asheghi, and K. E. Goodson, J. Appl. Phys. **109**, 084902 (2011).